Vol. 620: 47–62, 2019
https://doi.org/10.3354/meps12973

MARINE ECOLOGY PROGRESS SERIES
Mar Ecol Prog Ser

Published June 18

Climate change projections reveal range shifts of eelgrass *Zostera marina* in the Northwest Atlantic

Kristen L. Wilson*, Heike K. Lotze

Department of Biology, Dalhousie University, PO Box 15000, 1355 Oxford Street, Halifax, Nova Scotia B3H 4R2, Canada

ABSTRACT: Climate change is altering the distribution of marine species around the globe, including those providing critical 3-dimensional structure in important coastal habitats. We analysed how continued warming over the 21st century would affect the distribution of eelgrass *Zostera marina*, the dominant seagrass in the Northwest Atlantic and provider of essential ecosystem functions and services. We compiled presence-only occurrence records and built a species distribution model using Maxent to determine a present-day distribution, which was compared to physiological thresholds for eelgrass growth and reproduction. Present-day models were then projected to mid- (2040–2050) and end-century (2090–2100) using 2 contrasting emissions scenarios and different global climate models. Our projections suggest an average shift of the southern range limit by 1.41°N to the north under a strong mitigation scenario (RCP 2.6) and 6.48°N under a business-as-usual emissions scenario (RCP 8.5) by 2100, resulting in substantial loss of eelgrass habitat along the eastern coast of the USA. The northern edge shift was less certain, yet resulted in an expansion of total eelgrass habitat. To minimize the extent of eelgrass bed extinction and areas of reduced growth along the southern range, strong climate mitigation is critical. Moreover, warm-temperature stress in reduced-growth areas will greatly increase the susceptibility of eelgrass to other natural or anthropogenic stressors. Our results can inform coastal management and conservation planning to protect the essential structure, functions and services provided by eelgrass in a warming climate.

KEY WORDS: Seagrass beds · Coastal habitat · Climate warming · Maxent · Species distribution model (SDM) · Physiological threshold · Extinction · Range expansion

1. INTRODUCTION

Eelgrass *Zostera marina* is a temperate seagrass species with a circumglobal distribution along soft-sediment shorelines (Green & Short 2003). In the Northwest Atlantic, eelgrass is genetically distinct from other areas (Olsen et al. 2004), and is the dominant seagrass occurring from North Carolina to north of the Arctic Circle (Krause-Jensen & Duarte 2014, Olesen et al. 2015). Throughout this range, eelgrass occasionally co-exists with *Ruppia maritima* (widgeon grass) in low-saline environments (DFO, 2009). Along its southern distribution limit in North Carolina, eelgrass also coexists with *Halodule wrightii* (shoalgrass), which reaches its northern range limit there (Micheli et al. 2008). Eelgrass is an ecosystem engineer (Bos et al. 2007), creating complex 3-dimensional structure and providing critical food and habitat for many associated species (Schmidt et al. 2011). Eelgrass also plays significant roles in the storage and cycling of carbon and nutrients in coastal habitats (Schmidt et al. 2011) and the stabilization of coastlines by slowing currents and increasing sedimentation rates (Bos et al. 2007). As such, eelgrass is considered an ecologically significant species in Atlantic Canada, with a policy of no net loss (DFO 2009), and is protected by the Clean Water Act in the USA (Nelson 2009).

*Corresponding author: kristen.wilson@dal.ca

Since 1980, seagrass habitat has been lost globally at a rate of 110 km^2 yr^{-1} (Waycott et al. 2009), with eelgrass losing 1.4% of its habitat per year (Short et al. 2011), due to a range of natural and anthropogenic stressors. In the Northwest Atlantic, these stressors include coastal development, nutrient loading, reductions in water clarity, aquaculture impacts, the spread of invasive species, storm events, wasting disease, and, increasingly, climate change (Burdick et al. 1993, Lefcheck et al. 2017, Murphy et al. 2019). Ongoing climate change has already led to significant sea surface temperature (SST) increases since 1980 throughout the Northwest Atlantic (Barnett et al. 2001), resulting in northward shifts of SST isotherms (Hansen et al. 2006), and poleward shifts of marine species at a greater rate than terrestrial species (Poloczanska et al. 2013). In North Carolina, such increasing SST has resulted in decreases in eelgrass shoot density and biomass since 1985 (Micheli et al. 2008), and eelgrass has been further impacted by reductions in water clarity due to nutrient enrichment (Mallin et al. 2000). Decreasing water clarity has also been the long-term driver of eelgrass declines in Chesapeake Bay since the 1990s, disproportionally affecting deeper populations (Lefcheck et al. 2017) with some recent recoveries (Lefcheck et al. 2018); yet, significant die-offs recently occurred due to 2 marine heatwave events, in 2005 and 2010 (Moore et al. 2014). Similar trends have been observed along the entire northeastern seaboard of the USA (e.g. Beem & Short 2009, Costello & Kenworthy 2011).

Continued projected SST warming over the 21st century will likely result in further decreases in abundance, local extinction, and range shifts of eelgrass (Valle et al. 2014). One of the most common and well-developed approaches to quantify these potential range shifts utilizes species distribution models (SDMs) based on presence-only data (e.g. Jayathilake & Costello 2018, Wilson et al. 2019) or, if available, presence–absence data (e.g. Downie et al. 2013, Cacciapaglia & van Woesik 2018). Currently, SDMs of eelgrass have been performed for present-day distribution globally (Jayathilake & Costello 2018) and at regional scales (e.g. Valle et al. 2013, Kotta et al. 2014), with important implications for present-day eelgrass management. In addition, the response of eelgrass to projected climate change has been examined in the Baltic Sea (Kotta et al. 2014), and for the related *Zostera noltii* in the Northeast Atlantic (Valle et al. 2014), but not yet in the Northwest Atlantic, which includes rapidly warming areas such as the Gulf of Maine (Pershing et al. 2015). This is in contrast to other marine macrophytes, including several species of seaweed (e.g. Assis et al. 2018b, Wilson et al. 2019) that show southern edge extinction and range shifts, with substantial northern range expansions, corresponding to species-specific thermal tolerances along rocky shorelines in the Northwest Atlantic.

The goal of the present study was to understand how the distribution of eelgrass, the dominant macrophyte along soft-sediment shorelines in the Northwest Atlantic, may respond to climate change. We compiled eelgrass occurrence records and used a correlative presence-only SDM to estimate the present-day distribution of eelgrass, and then projected how this distribution may shift under mild to strong climate change scenarios over the 21st century. In addition, we compared the predicted present-day and projected future habitat areas to physiological thresholds (PTs) for growth and reproduction to evaluate the reliability of model results. We hypothesized that eelgrass would experience a northward range expansion, with losses along its southern edge depending on the strength of warming. We discuss the magnitude of expected range shifts, and how they will impact the critical ecosystem structure, functions, and services eelgrass provides to marine ecosystems and human well-being.

2. MATERIALS AND METHODS

2.1. Present-day *Zostera marina* distribution

In the Northwest Atlantic, eelgrass *Zostera marina* occurs from North Carolina (~34° N; Micheli et al. 2008) to Greenland (~64° N; Olesen et al. 2015), with noticeable absences from Delaware Bay and the northern shore of the Bay of Fundy (Green & Short 2003). In western Greenland, eelgrass has been observed at 64° N, with unconfirmed reports as far north as 69° N (Olesen et al. 2015). In eastern Canada, eelgrass is known as far north as Lake Melville in Labrador (~54° N; DFO, 2009), with an unconfirmed distribution along the Labrador coast up to Ungava Bay (Cottam & Munro 1954). Eelgrass is also present in James Bay (Lalumière et al. 1994) and Hudson Bay, with some older reports of eelgrass occurring up to 61° N along the low-lying marshes of western Hudson Bay (Porsild 1932). As eelgrass in the Northwest Atlantic is genetically distinct from other areas (Olsen et al. 2004), the Northwest Atlantic was considered a relevant study area, as it can be considered a unique biogeographic region.

To inform the SDMs, presence-only occurrence records were collected for eelgrass throughout the described range in the Northwest Atlantic as absence records were not consistently available. Geographic coordinates of known locations of eelgrass beds with the year that eelgrass was observed were collected via a literature search, correspondence with other research groups, local ecological knowledge, citizen science, state-wide mapping projects, and online databases (Tables S1–S3 in Supplement 1 at www.int-res.com/articles/suppl/m620p047_supp1.xls). To ensure occurrence records used in model building reflected the environmental conditions at the time, only records since 2000 were included in the analysis (see Section 2.2). Yet, due to the inaccessibility and lack of data in northern areas, we also used records from 1980 to 2000 in areas north of 47° N (Wilson et al. 2019), with 1980 chosen as a cut-off as this was the first year with significant increases in SST in the Northwest Atlantic (Barnett et al. 2001). It was assumed that any warming in this area would only facilitate northward range shifts, and that other anthropogenic threats, such as eutrophication-induced light reduction, would be minimal due to low human population density. Occurrence records were processed to remove duplicate records within an environmental grid cell, and projected into the Behrmann cylindrical equal-area projection (see Section 2.2) using ArcGIS® v.10.5 (ESRI).

2.2. Present and future environmental data

The marine environmental dataset Bio-Oracle 2.0 was used to represent present-day conditions (Tyberghein et al. 2012, Assis et al. 2018a). This global data set provides long-term averages (LTA) from 2000 to 2014, in Behrmann cylindrical equal-area projection, at a 7 km pixel resolution. The environmental data were cropped from 32° to 84° N and 42° to 95° W, and all pixels >100 km from shore and in water depths >12 m were excluded from analysis within the statistical environment R (R Core Team 2018) using the 'sdmpredictors' package (Bosch et al. 2018). The maximum bathymetry layer from Bio-Oracle 2.0 was used to delineate water depth, which is based on GEBCO bathymetry data. This provided a background area for model building that is biologically and geographically relevant, as it included the entire latitudinal spread of a genetically distinct population encompassing common to extreme conditions, in addition to closely matching eelgrass observed present-day distribution in the Northwest Atlantic (Barve et al. 2011, Acevedo et al. 2012).

We considered a large range of variables known to affect eelgrass distribution, that included the LTA mean of the maximum (i.e. warmest) month (M-max) and the minimum (i.e. coolest) month (M-min) for SST, sea surface salinity (SSS), and sea ice coverage (SIC), and LTA yearly minimum and maximum (Y-max, Y-min) for diffuse attenuation (DA) as provided by the Bio-Oracle 2.0 data set, to build our SDM. This incorporated the range of environmental conditions eelgrass encounters during a year and all variables are known to impact eelgrass distribution (Lee et al. 2007, Nejrup & Pedersen 2008, Olesen et al. 2015). SIC M-min was included to delineate the southern extent of year-round ice. To ensure the variables included in model building were uncorrelated, the variable inflation factor (VIF) was examined between all variables, and variables were removed in a stepwise fashion until all had a VIF <10 (Naimi et al. 2014). See Table S1 in Supplement 2 at www.int-res.com/articles/suppl/m620p047_supp2.pdf for summary metrics for each environmental variable and Table S2 in Supplement 2 for a Pearson correlation matrix.

To project onto the future climate, we incorporated 2 global climate models from CMIP5 (Taylor et al. 2012): GFDL-ESM2M projecting lower (GFDL hereafter; Dunne et al. 2012) and IPSL-CM5A-LR projecting higher (IPSL hereafter; Dufresne et al. 2013) levels of SST warming (Bopp et al. 2013), thus encompassing a range of mild to strong warming. We calculated an LTA for present-day (2006–2015), mid-century (2040–2050), and end-century (2090–2100) for 2 representative concentration pathways (RCPs): a low carbon concentration and strong mitigation scenario (RCP 2.6) and a high carbon concentration business-as-usual scenario (RCP 8.5; Moss et al. 2010). Present-day was chosen to begin in 2006 as this is the year climate model data switch from historical runs to future projections forced by each RCP scenario. We then determined a relative change in each variable, as there are uncertainties between present-day climate model data and present-day observed data. The relative changes were calculated by subtracting the mid-century LTA (2040–2050) or end-century LTA (2090–2100) from the present-day LTA (2006–2015) for each of the climate models and RCP scenarios. These relative changes (anomalies) were then added to the present-day observed value to determine a new value for mid- or end-century. This was done for the SST, SSS, and SIC variables. All future projections hold DA at present-day values as no future layers of DA were available.

To calculate mid-century eelgrass range shifts, the predicted present-day range limit was subtracted

from the projected mid-century range limit. Range shifts from mid- to end-century were calculated by subtracting the projected mid-century range limit from the projected end-century limit, and total range shifts were calculated by subtracting the predicted present-day range limit from the projected end-century range. For the southern edge, we calculated quantitative range shifts in terms of degree and kilometre shifts. However, due to northern edge uncertainties (see Section 4.2), we only provide a qualitative discussion about eelgrass distribution in northern areas, and changes in northern range limits are reflected in changes in habitat area.

2.3. SDM building, evaluation and projection

The correlative SDM was built with Maxent v.3.3.3k (Phillips et al. 2004, 2006) in the statistical environment R (R Core Team 2018) using the 'dismo' package (Hijmans et al. 2017). Maxent was chosen as it is the top-performing presence-only modelling algorithm (Elith et al. 2006). Eelgrass present-day distribution was built using *k*-fold cross-validation with $k = 5$, which divides the occurrence records into 5 data sets, and each is used in testing once and training $k-1$ times (Kohavi 1995). We allowed smooth functions (linear, quadratic, and hinge feature classes) to increase the robustness of our predictions (Elith et al. 2010), a maximum of 5000 iterations, and thresholded the continuous model output with a threshold that maximizes the sum of test sensitivity and specificity (MSTSS; Liu et al. 2016). Model performance was evaluated using the area under the curve (AUC) of the receiver operator characteristics curve, and a one-tailed binomial test (Phillips et al. 2006). Model complexity was reduced using a jackknife test to remove environmental variables based on balancing the response of training and test gain (Wilson et al. 2019). The SDM was run with all uncorrelated predictor variables, and the variable with the smallest decrease in test gain was removed. This was repeated until there was a significant decrease in training gain based on 95% confidence intervals to balance the importance of variables for model training and testing.

After determining the 'best' SDM for eelgrass using the *k*-fold cross validation, the best model was rerun using all occurrence records (typically 2000 onwards, except 1980s onwards in the Arctic) to ensure the model was trained on the full range of environmental conditions ($k = 1$). See Figs. S1 and S2 in Supplement 2 for the individual and combined response curves per environmental variable for this model. The model output was thresholded using the average MSTSS threshold from the cross-validation runs. Exploratory analysis showed the range limits predicted from using all occurrence records were almost identical to the average range limits provided from the *k*-fold cross-validation models. This best model, with the full set of occurrence records, was projected onto the future climate for mid- (2040–2050) and end-century (2090–2100) at RCP 2.6 and 8.5. All runs were clamped to avoid training from data outside the species' current range (Elith et al. 2010).

2.4. Physiological thresholds

To incorporate empirical evidence for our projected range shifts of eelgrass, we conducted a literature search to determine the response of eelgrass to varying SST throughout its global distribution (Table S3 in Supplement 2). Throughout its present-day range in the Northwest Atlantic, eelgrass is exposed to maximum summer SSTs above 30°C in shallow estuaries in North Carolina (Jarvis et al. 2012) and maximum summer SSTs as low as 10°C in western Greenland (Olesen et al. 2015). This broad range of temperature tolerance across latitudes results in highly varied optimal SST for growth and survival that is often dependent on latitude (Lee et al. 2007). Yet, on average globally and in the Northwest Atlantic, eelgrass experiences optimal growth at ~15.3°C, with optimal photosynthesis at ~23.3°C (Lee et al. 2007). Eelgrass generally grows well at SSTs from 10 to 25°C, with growth reductions above 25°C (DFO 2009), and SSTs above 30°C have been proposed as a critical threshold as eelgrass experiences stunted growth and some mortality (Moore et al. 2012). Eelgrass has optimal flowering and seed recruitment from 15 to 20°C (De Cock 1981), with limited capacity for sexual reproduction below 10°C (Churchill & Riner 1978). Cooler temperatures do not limit eelgrass persistence as eelgrass regularly overwinters in areas with winter sea ice (Lalumière et al. 1994, Olesen et al. 2015) and has some resistance to freezing (Biebl & McRoy 1971).

The SST M-max layer for present-day and future climate was reclassified based on the following PTs: limited sexual reproduction below 10°C, good growth from 10 to 24°C, growth reductions from 25 to 29°C, and stunted growth and partial mortality above 30°C. Along the eelgrass southern distribu-

tion limit, SST M-max is an indicator of growth and survival physiological tolerances, and along northern distribution limits it is an indicator of sexual reproductive limits (see Section 4.1). Exploratory analysis showed that SST M-max was typically within 1°C, to a maximum of 3°C, of SST Y-max for all climate models south of Labrador, with differences of up to 7°C throughout the Arctic for RCP 8.5 at end-century. Therefore, SST M-max is comparable to SST Y-max along the species' southern edge. Furthermore, marine macrophyte heat tolerance depends on the length of time the species is exposed to extreme temperatures, and an LTA of monthly mean SST of the warmest month on average (SST M-max) is a better indicator of average conditions as opposed to a heatwave event only lasting a few days, which would be better reflected by SST Y-max.

The PTs are not incorporated into the building of the Maxent model. Instead, this reclassified layer was overlaid onto the predicted/projected eelgrass distribution from the correlative SDM (Maxent) to evaluate the reliability of results. Areas of predicted habitat based on the correlative SDM, corresponding to PTs for good growth, were likely to contain suitable habitat, while areas corresponding to PTs for reduced or stunted growth were less likely to contain suitable habitat and may be more susceptible to interactive effects of warming and other environmental stressors (Wilson et al. 2019). The incorporation of empirical data with PTs provides more robust present-day predictions and future projections of species distributions, and highlights areas where future projections may be uncertain (e.g. Martínez et al. 2015, Serebryakova 2017, Wilson et al. 2019). This incorporation is not done in model building, but rather to evaluate the denoted habitat as predicted/projected by Maxent.

3. RESULTS

3.1. Model building and evaluation

We retained 8 predictor variables to be used in the model selection process that were uncorrelated based on a VIF <10 and a Pearson correlation coefficient <0.9 (Table 1; Table S2 in Supplement 2). The model with the highest average regularized training gain was Drop 1, with Drop 2 being the last model to have a similar training gain based on 95% confidence intervals (Fig. 1). Therefore, the model with SIC M-min and DA Y-max removed produced the 'best' model (Table 1). During model building, SST M-min was the most important variable for predicting eelgrass presence based on test gain (Table 1). For the best model (Drop 2), SST M-max, followed by SST M-min and SIC M-max were the most important predictor variables based on training gain, with SST M-min followed by SSS M-max being the most important predictor variables based on training AUC (Table 2). Therefore, SST M-max and SST M-min appeared to be the most important predictor variables for indicating eelgrass presence. In addition, the cross-validated and full model had similar training gain, AUC, percent contributions and permutation importance between variables, indicating high similarities between the 2 runs. Lastly, the average test AUC was >0.9, with the binomial p-value <0.01 for the MSTSS threshold, indicating good model performance on test data.

Table 1. Description and abbreviations of environmental variables used in model building with their variable inflation factor (VIF). All are long-term averages of the yearly maximum or minimum (Y-max, Y-min) or mean of the highest or lowest month (M-max, M-min) from 2000 to 2014. Variable order indicates order removed by test gain and shows which environmental variables were included in each model. For instance, Drop 6 includes both SST M-min and SSS M-max. **Bold** environmental variables were used in the best model (Drop 2), which was determined using 95% confidence intervals (see Fig. 1). DA: diffuse attenuation; SIC: sea ice coverage; SSS: sea surface salinity; SST: sea surface temperature

Variable	Abbreviation	VIF	Model
Mean sea ice coverage of the lowest month on average	SIC M-min	1.01	Drop 0
Yearly maximum diffuse attenuation value	DA Y-max	4.64	Drop 1
Mean sea surface temperature of the warmest month on average	**SST M-max**	**6.80**	**Drop 2**
Yearly minimum diffuse attenuation value	**DA Y-min**	**3.16**	**Drop 3**
Mean sea ice coverage of the highest month on average	**SIC M-max**	**2.78**	**Drop 4**
Mean sea surface salinity of the freshest month on average	**SSS M-min**	**5.61**	**Drop 5**
Mean sea surface salinity of the saltiest month on average	**SSS M-max**	**5.83**	**Drop 6**
Mean sea surface temperature of the coolest month on average	**SST M-min**	**3.29**	**Drop 7**

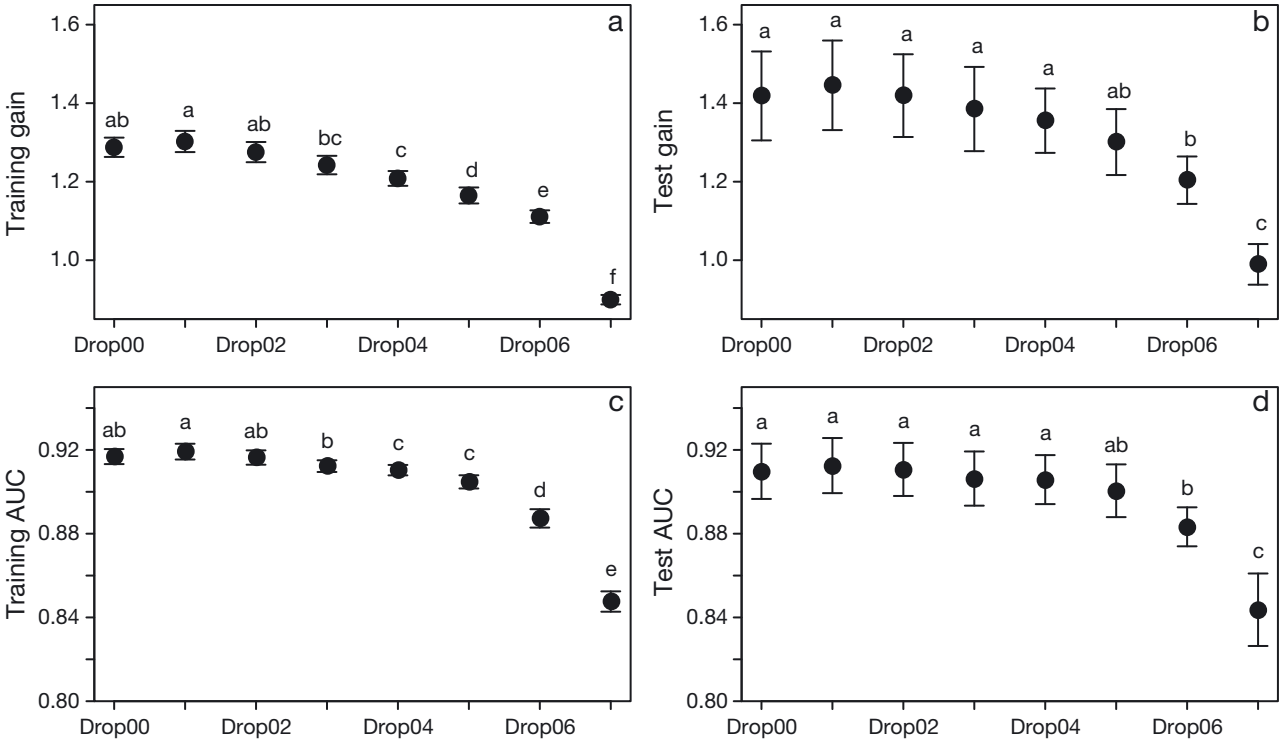

Fig. 1. Average training (left column) and test (right column) for (a,b) model gain and (c,d) area under the curve (AUC), showing 95% confidence intervals per 5-fold ($k = 5$) cross-validation model runs used to determine the best model (Drop 2). Different letters indicate a significant difference based on results of the 95% CI tests

Model metric	Cross-validation (mean ± SE)	Full
Training		
Regularized gain	1.28 ± 0.01	1.26
AUC	0.92 ± 0.00	0.91
Test		
Gain	1.41 ± 0.04	NA
AUC	0.91 ± 0.01	NA
Maximizing the sum of test sensitivity and specificity		
Logistic threshold	0.33 ± 0.01	NA
Binomial p-value	p < 0.01	NA
Percent contribution (%)		
SST M-max[a]	50.31 ± 1.71	51.47
DA Y-min	2.22 ± 0.24	1.93
SIC M-max[a]	11.86 ± 0.96	12.78
SSS M-min[a]	1.83 ± 0.20	2.32
SSS M-max[a]	7.92 ± 0.42	5.87
SST M-min[a]	25.84 ± 2.47	25.63
Permutation importance (%)		
SST M-max[a]	8.71 ± 0.73	9.64
DA Y-min	1.60 ± 0.21	1.29
SIC M-max[a]	5.33 ± 0.16	5.65
SSS M-min[a]	8.29 ± 0.27	7.59
SSS M-max[a]	22.32 ± 0.61	22.85
SST M-min[a]	53.74 ± 0.83	52.99

[a]Variable was replaced with projected future climate data in model projections

Table 2. Different model metrics to evaluate the best model (Drop 2) for the cross-validation runs ($k = 5$) and full run with all occurrence records as training values ($k = 1$). Percent contribution shows how a variable influenced training gain per iteration. Permutation importance shows how removing a variable decreased training area under the curve (AUC) per iteration. Variables are listed by the order in which they were removed from the model (see Table 1)

3.2. Eelgrass present-day distribution

Using the full set of occurrence records (507 pixels with eelgrass presence from 9876 records) to train the model, a total area of 185 465 km^2 was predicted to be suitable eelgrass habitat (Fig. 2, Table 3). This is a maximum value as the entire area within a 7 km^2 pixel may not contain suitable habitat, but we present this value to indicate the magnitude and direction of change in future projections. A present-day southern distribution limit was predicted at 33.85° N in North Carolina, with the most southern occurrence record at 34.63° N. In this southern range, eelgrass was exposed to SSTs corresponding to reduced growth within Chesapeake Bay and along the North Carolina coastline, corresponding to

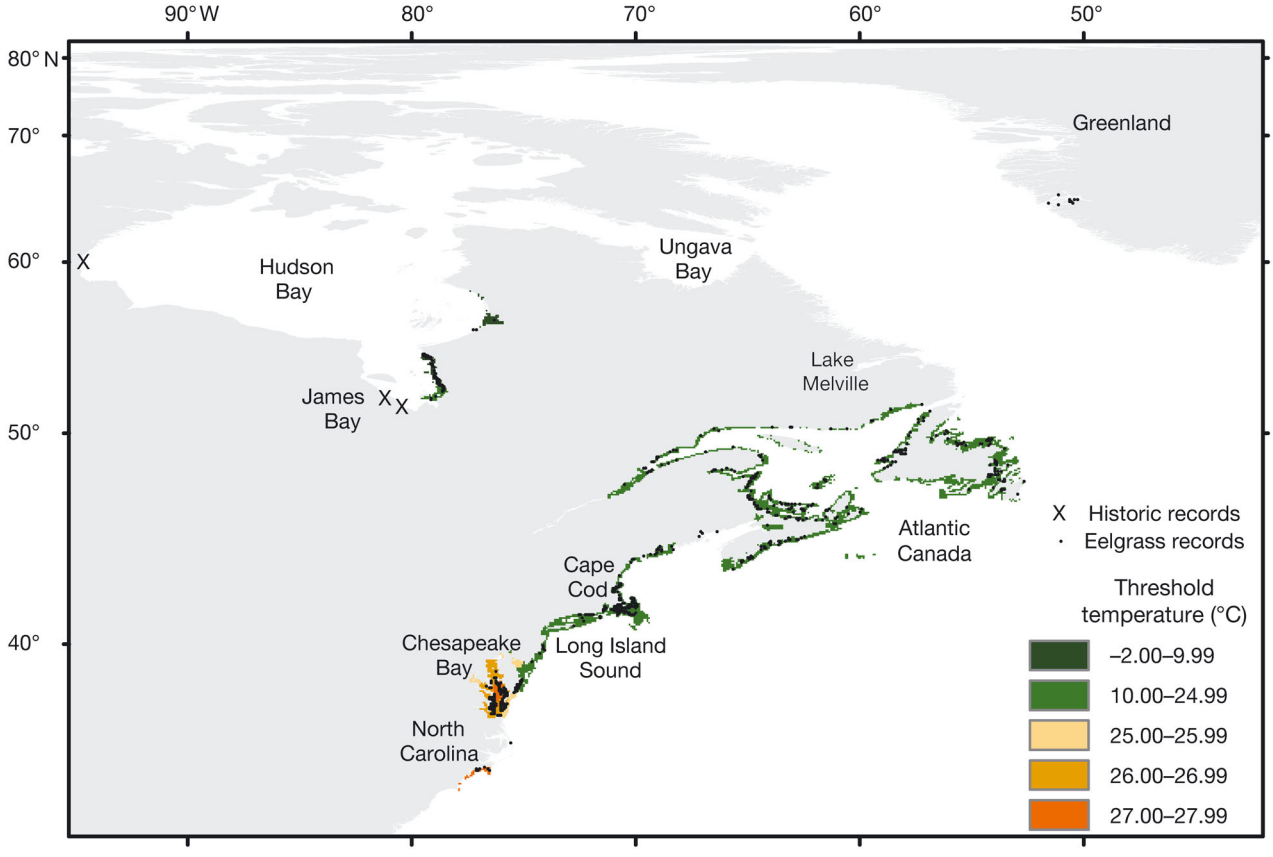

Fig. 2. Eelgrass *Zostera marina* location of occurrence records in the Northwest Atlantic and predicted present-day distribution based on all environmental data included in the best model. Historic records in northern areas are older than 1980 and were not included in present-day predictions nor used in any data analysis. Physiological thresholds (based on SST M-max) were overlaid to show areas of limited sexual reproduction (dark green, <10°C), good growth (green, 10.00–24.99°C), and reduced growth (orange-red, 25.00–27.99°C). No temperatures corresponding to reduced growth at 28.00–29.99°C or stunted growth and partial mortality (≥30°C) were observed

12.60% (23 373 km^2) of the overall predicted habitat. All occurrence records occurred in SST <30°C, indicating a strong correlation with the PTs. Predicted eelgrass habitat continues northward almost continuously to southern Labrador at 51.58° N, with the northernmost confirmed occurrence record at 51.50° N. Within the Hudson Bay region, present-day occurrence records exist north to 56.29° N, and predicted habitat was limited to a continuous stretch along the eastern shores of Hudson Bay up to 58.10° N; however, some older historic eelgrass records suggest that eelgrass may also occur along the southern and western Hudson Bay (61.10° N, 94.10° W and 51.5° N, 80.50° W; Fig. 2). In western Greenland, no habitat was predicted despite the known occurrence of eelgrass to 64.81° N. The continuous (non-thresholded) present-day distribution is shown in Fig. S3 in Supplement 2.

3.3. Eelgrass distribution under a strong mitigation scenario

Under RCP 2.6, the southern range limit of eelgrass was projected to shift farther north by mid-century, with GFDL (low warming) and IPSL (strong warming) projecting the same range shift (Figs. 3 & 4). From mid- to end-century, GFDL projected some southern range expansion and IPSL projected no change; therefore, eelgrass is likely to experience an average shift of its southern range by 1.41° N (147 km) to the north by the end of the 21st century (Table 3). This corresponded to a loss of habitat within North Carolina. This habitat loss by end-century did not affect areas of good growth (<25°C) but decreased the areas of reduced growth along eelgrass' southern range from 12.60% at present-day to 11.70% for GFDL (25 137 km^2) and 6.43% for IPSL (14 847 km^2;

Table 3. Projected range shifts (RS, °N; *km*, *in italics*) within each climate model (GFDL, IPSL) and their average (Avg, **bolded**) response are shown based on relative changes in sea surface temperature, sea surface salinity, and sea ice coverage. The new projected habitat area and its allocation to reduced growth (RG), and the magnitude and direction of change (square brackets, *in italics*) in area and RG from present-day to mid-century, mid-century to end-century, and present-day to end-century (total) are shown. Note that the area and RG are the same for end-century and total, but the magnitude of change is different. Note that all area measurements are a maximum possible value, as not all habitat within a 49 km^2 may contain suitable habitat

Climate model	RCP 2.6 RS[a] (°N; *km*)	RCP 2.6 Area[b] (km^2)	RCP 2.6 RG[c] (%)	RCP 8.5 RS[a] (°N; *km*)	RCP 8.5 Area[b] (km^2)	RCP 8.5 RG[c] (%)
Mid-century						
GFDL	3.01	217 952	10.54	3.01	202 811	6.40
	315	[*32 487*]	[*–2.06*]	*315*	[*17 346*]	[*–6.20*]
IPSL	3.01	204 624	7.78	3.01	190 463	6.20
	315	[*19 159*]	[*–4.82*]	*315*	[*4 998*]	[*–6.40*]
Avg	**3.01**	**211 288**	**9.16**	**3.01**	**196 637**	**6.30**
	315	**[*25 823*]**	**[*–3.44*]**	***315***	**[*11 172*]**	**[*-6.30*]**
End-century						
GFDL	–3.21	214 865	11.70	3.49	253, 918	2.91
	–336	[*–3 087*]	[*1.16*]	*350*	[*51 107*]	[*–3.49*]
IPSL	0.00	230 790	6.43	3.42	226 821	10.52
	0	[*26 166*]	[*–1.35*]	*343*	[*36 358*]	[*4.32*]
Avg	**–1.61**	**222 828**	**9.07**	**3.46**	**240 370**	**6.72**
	–168	**[*11 540*]**	**[*–0.10*]**	***347***	**[*43 733*]**	**[*0.42*]**
Total						
GFDL	–0.20	214 865	11.70	6.51	253 918	2.91
	–21	[*29 400*]	[*–0.90*]	*665*	[*68 453*]	[*–9.69*]
IPSL	3.01	230 790	6.43	6.44	226 821	10.52
	315	[*45 325*]	[*–6.17*]	*658*	[*41 356*]	[*–2.08*]
Avg	**1.41**	**222 828**	**9.07**	**6.48**	**240 370**	**6.72**
	147	**[*37 363*]**	**[*–3.54*]**	***662***	**[*54 905*]**	**[*–5.89*]**

[a]For reference, the predicted present-day distribution southern range limit is 33.85° N; [b]For reference, the predicted present-day habitat area is 185 465 km^2; [c]For reference, the predicted allocation of present-day habitat to reduced growth is 12.60 %

3.4. Eelgrass distribution under a business-as-usual scenario

The projected 21st century range shift for eelgrass under RCP 8.5 was identical between GFDL and IPSL by mid-century, although GFDL projected a slightly greater range shift by end-century (Table 3). On average, eelgrass was projected to experience a 6.48°N (662 km) northward range shift of the southern edge by 2100, suggesting a loss of eelgrass habitat south of Long Island Sound (Figs. 3 & 4). Moreover, IPSL and GFDL projected the proportion of eelgrass habitat corresponding to reduced growth to decrease from 12.60 % in present-day to 10.52 % (23 863 km^2) and 2.91 % (7399 km^2), respectively, by 2100 in its southern range (Table 3). In the north, both GFDL and IPSL again projected range expansions along the western shores of Hudson Bay, up the Labrador Coast to slightly past Lake Melville, patchy habitat into the many islands throughout the Canadian Arctic, with no expansion to western Greenland (Figs. 3 & 4). Therefore, by 2100, eelgrass may experience some northern range expansions, with changes in the proportion of habitat corresponding to limited reproduction. Overall, the projected range shift of eelgrass resulted in a greater increase in total habitable area compared to RCP 2.6 (Table 3). The continuous (non-thresholded) future-day distribution is shown in Figs. S4 & S5 in Supplement 2.

Table 3). In the north, both GFDL and IPSL projected range expansions along the western shores of Hudson Bay, where historic records have also suggested eelgrass presence (Fig. 2), and Ungava Bay by mid-century, persisting to end-century, while no range expansion was projected to western Greenland (Figs. 3, 4). Therefore, by 2100 under RCP 2.6, eelgrass may experience small northern range expansions, but this generally corresponded to habitat with limited sexual reproduction. Overall, the projected range shift of eelgrass would result in an increase of the total habitat area from present-day (Table 3). The continuous (non-thresholded) future-day distribution is shown in Figs. S4 & S5 in Supplement 2.

4. DISCUSSION

Our goal was to understand how continued climate change may impact the distribution of eelgrass *Zostera marina* in the Northwest Atlantic. To do so, we built a presence-only SDM and compared the predicted distribution to PTs for growth and reproduction. We found that the total predicted present-day area of eelgrass habitat ranged from ~33° N to ~70° N. We then projected the SDM to mid- and end-century us-

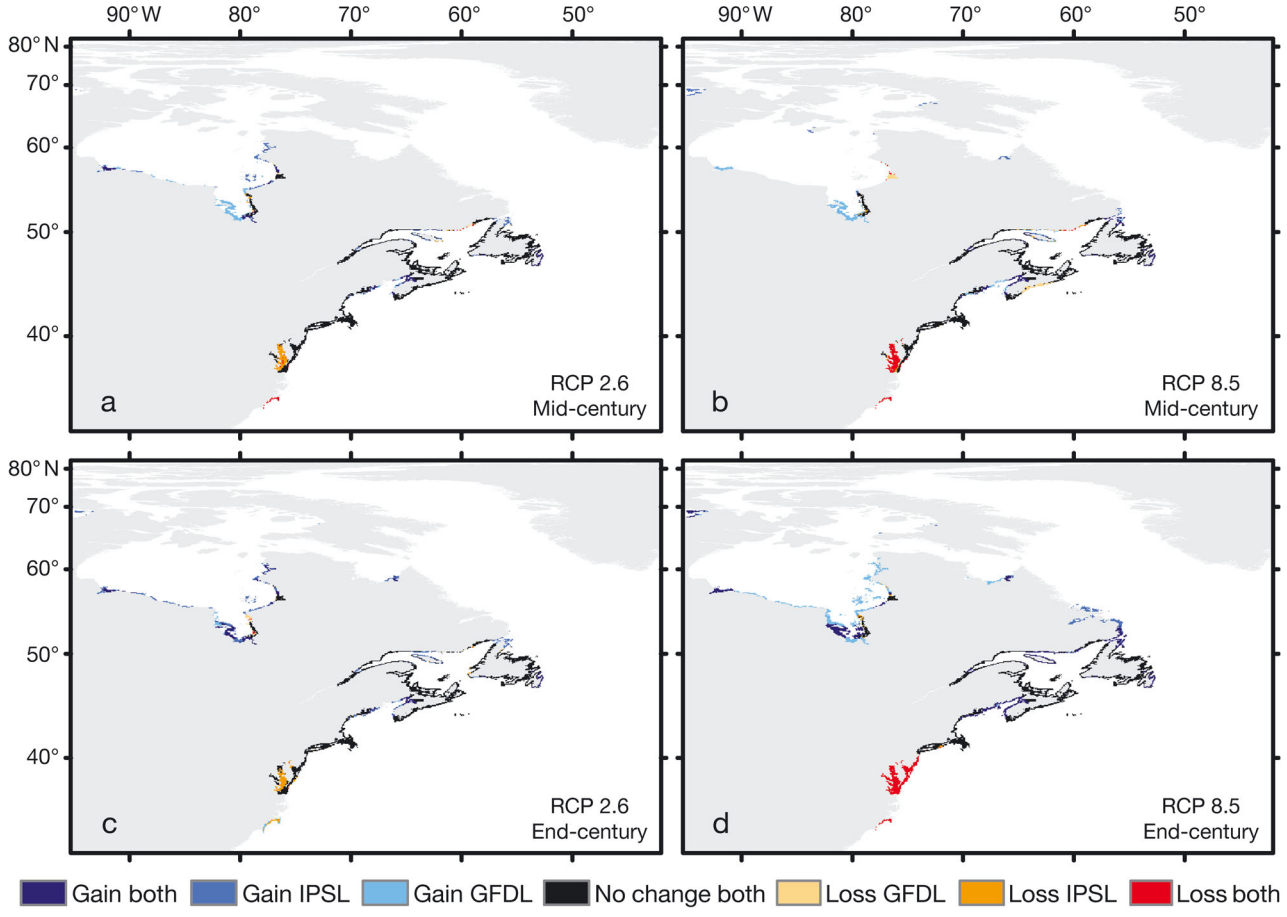

Fig. 3. Eelgrass *Zostera marina* projected (a,b) mid-century and (c,d) end-century distribution based under RCP 2.6 (left column) and RCP 8.5 (right column). Habitat gain (expansion) from present-day distribution is indicated in shades of blue; habitat loss (contraction) in shades of orange to red. To highlight consensus in projections, 'Both' indicates changes projected by both GFDL-ESM2M and IPSL-CM5A-LR. To highlight areas of uncertainty, GFDL refers to changes projected under GFDL-ESM2M only (low warming) and IPSL refers to changes projected under IPSL-CM5A-LR only (strong warming). No change from present-day for both climate models is indicated in black

ing different climate models and emissions scenarios. Future projections suggested northward shifts of both the southern and northern range limits (edges), resulting in extinctions of eelgrass along its southern range limit and expanding eelgrass beds in the Arctic. Overall, these range shifts aligned well with our PTs, thus increasing our confidence in model projections. The range shifts corresponded to increases in total habitat area and decreases in habitat areas with reduced growth, while changes in habitat areas with limited reproduction varied with climate scenario. No areas corresponding to SST for stunted growth and partial mortality were denoted as suitable habitat. We discuss the consequences of these projected shifts for the ecosystem structure, functions and services provided by eelgrass, and the implications for management and conservation.

4.1. Factors impacting eelgrass distribution

Light availability is the dominant factor affecting eelgrass growth, followed by water temperature and nutrient availability (Lee et al. 2007). Therefore, it was surprising that DA, an indicator of water clarity and, consequently, light availability, was one of the least important predictor variables for eelgrass presence. Interestingly, SST M-min was the most important predictor variable, over SST M-max. Generally, maximum SST drives species' southern range limits as temperatures exceed growth and survivorship thresholds (Wilson et al. 2019), while minimum SST drives northern range limits, and this was a more important predictor for eelgrass distribution in our study.

Along the northern range limit of eelgrass in Greenland, leaf growth rates are reduced, but total

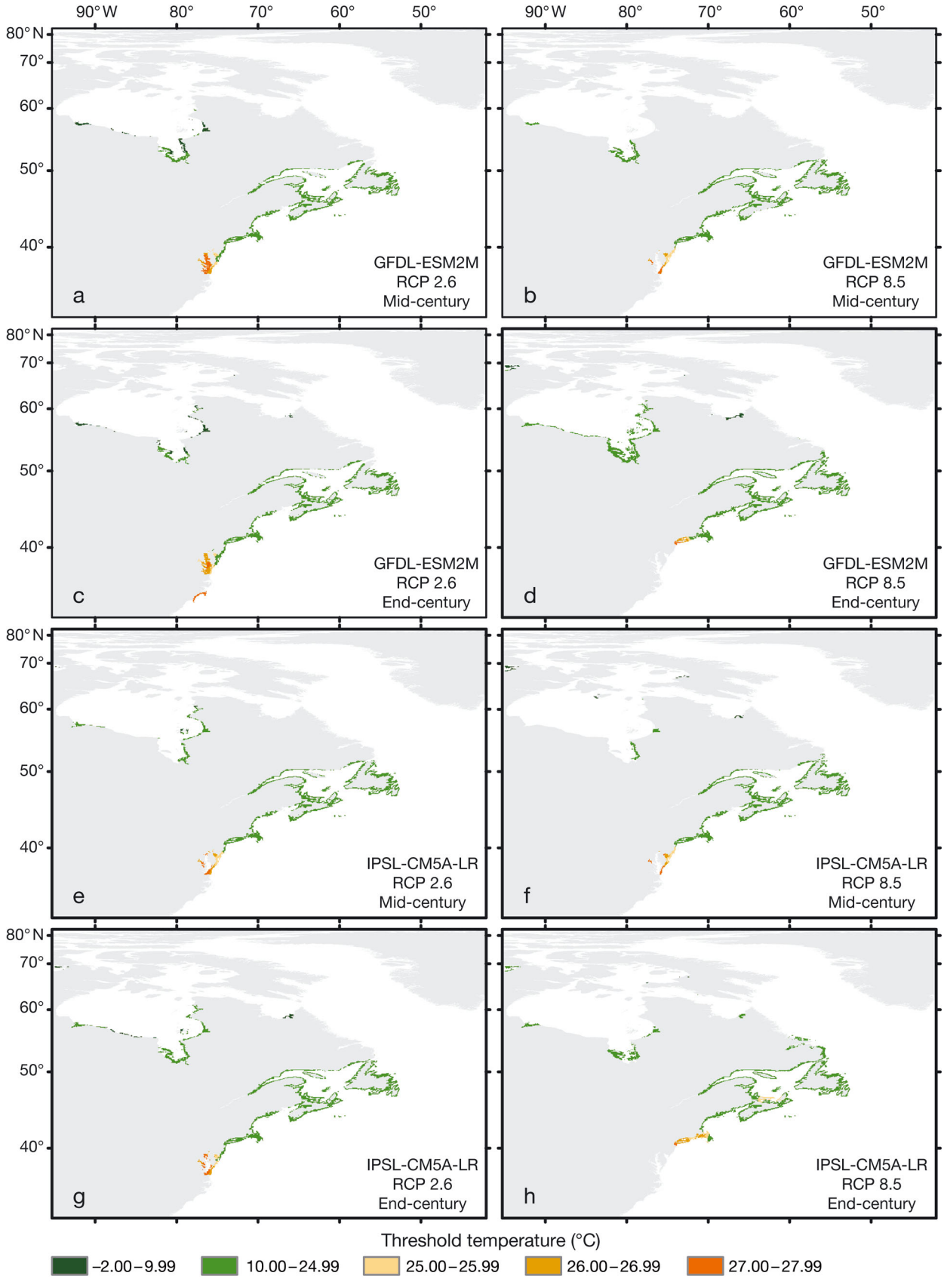
90° W
80°
70°
60°
50°
80° N
70°
60°
50°
40°
a
GFDL-ESM2M
RCP 2.6
Mid-century
b
GFDL-ESM2M
RCP 8.5
Mid-century
c
GFDL-ESM2M
RCP 2.6
End-century
d
GFDL-ESM2M
RCP 8.5
End-century
e
IPSL-CM5A-LR
RCP 2.6
Mid-century
f
IPSL-CM5A-LR
RCP 8.5
Mid-century
g
IPSL-CM5A-LR
RCP 2.6
End-century
h
IPSL-CM5A-LR
RCP 8.5
End-century
Threshold temperature (°C)
−2.00–9.99
10.00–24.99
25.00–25.99
26.00–26.99
27.00–27.99

Fig. 4. Eelgrass *Zostera marina* projected (a,b,e,f) mid-century and (c,d,g,h) end-century distribution under RCP 2.6 (left column) and RCP 8.5 (right column) from GFDL-ESM2M (a–d) and IPSL-CM5A-LR (e–h). Physiological thresholds (based on SST M-max) were overlaid to show areas of limited sexual reproduction (dark green, <10°C), good growth (green, 10.00–24.99°C), and reduced growth (orange-red, 25.00–27.99°C). No temperatures corresponding to reduced growth at 28.00–29.99°C or stunted growth and partial mortality were observed (≥30°C)

standing leaf biomass is comparable to that of more temperate populations (Olesen et al. 2015). Furthermore, eelgrass is thought to be metabolically active during Greenland winters, and Alaskan populations exhibit detectable photosynthesis and respiration at 0°C (Biebl & McRoy 1971). Therefore, although growth rates of eelgrass may be reduced at higher latitudes, low temperatures are not limiting eelgrass persistence. Instead, the northern range limit of eelgrass appears to be set by its capacity for sexual reproduction. Eelgrass flowering and seed maturation can only occur at temperatures of 10–15°C (Churchill & Riner 1978), while viable seeds can remain dormant to overwinter at temperatures of 0°C (Infantes et al. 2016), and seed germination occurs in spring or fall at temperatures as low as 5°C (Abe et al. 2008). In particular, the temperature requirements for eelgrass flowering and seed maturation appear to drive the northern distribution limit, as seed recruitment in Greenland populations is limited to years with unseasonably warm summers (Olesen et al. 2015). Currently, the Godthåbsfjord fjord system at ~64.5° N has been suggested to be the northern limit for sexual reproduction, and large clonal patches are common throughout this fjord system with reproductive shoots present only in the inner, warmer sections. As SST continues to rise, leading to an increase in the number of days above 10°C, eelgrass will likely have an increased capacity for sexual reproduction, which may help to facilitate northward range shifts. Similarly, increases in the number of days above a critical low-temperature reproductive threshold has led to significant increases in terrestrial plant species in Antarctica (Hughes 2000).

4.2. Eelgrass present-day distribution and projected range shifts

Currently, eelgrass exists south to the Bogue Sound–Back Sound region of North Carolina (Micheli et al. 2008), which corresponded to our most southern occurrence record at ~34° N. Yet our present-day SDM predicted eelgrass habitat further south to 33° N, thus our projections may be slightly underestimating the southern edge range shift by ~1°. Along this southern distribution limit, eelgrass has developed a unique life history strategy, depending on a combination of annual and perennial life cycles allowing for yearly vegetative/asexual growth and sexual reproduction to maintain eelgrass populations that are regularly exposed to high temperature stress >30°C (Jarvis et al. 2012). This temperature stress also results in winter–spring being the prime growing season, reaching peak eelgrass biomass, with large losses of aboveground biomass during warm summer months (Micheli et al. 2008). In contrast, more northern populations of eelgrass reach peak biomass in late summer (Clausen et al. 2014), and the perennial life cycle is dominant (Moore et al. 2012, Olesen et al. 2015).

Under a strong carbon emissions mitigation scenario (RCP 2.6) with mild warming, eelgrass was projected to experience an average increase of suitable eelgrass habitat along the Northwest Atlantic by 2100 based on the relative average response of GFDL and IPSL. However, eelgrass will also likely experience a small southern range shift by 2050, which will persist to 2100, and corresponds to loss of eelgrass habitat within North Carolina. As eelgrass in North Carolina is considered a separate ecotype from more northern populations, with greater tolerance to higher SST, any loss of genetic diversity from this trailing edge population may increase the susceptibility of eelgrass in the Northwest Atlantic to the impacts of continued warming (Mallin et al. 2000, Jueterbock et al. 2016).

Currently, seagrasses in North Carolina follow strict zonation patterns, with shoalgrass occurring within the intertidal zone and eelgrass persisting below the mean low water mark (Micheli et al. 2008). Transplant experiments have shown that shoalgrass can persist in areas of greater depth if eelgrass habitat were to disappear, but with reduced diversity and abundance of associated infauna and epifauna (Micheli et al. 2008). Therefore, while shoalgrass may mitigate some of the impacts from the loss of eelgrass habitat, there will be a net loss of ecosystem functions and services following the projected extirpation of eelgrass in North Carolina. This further applies to any ecosystem functions facilitated by northward shifts of shoalgrass with continued climate change. Furthermore, despite significant increases in SST, and associated losses of eelgrass within North Carolina, shoalgrass has yet to naturally colonize historic areas of eelgrass habitat (Micheli et al. 2008).

Under a business-as-usual carbon emissions scenario (RCP 8.5) with strong warming, it is highly probable that eelgrass will experience extirpation in North Carolina and Chesapeake Bay as well as a southern range shift to Long Island Sound by 2100. This is in contrast to small-scale bio-optical models that have predicted that eelgrass may persist with increasing temperatures in Chesapeake Bay given improved water clarity (Zimmerman et al. 2015) due to successful long-term water quality improvements that have reduced nutrient loading and increased submerged aquatic vegetation (Lefcheck et al. 2018). In particular, the outer Delmarvian Bays experience cold-water upwelling during the summer, which had protected eelgrass beds from previous heatwave events (Moore et al. 2012). Eelgrass in Chesapeake Bay has already experienced a 'squeeze effect', where the vertical zonation has been reduced, with maximum bed depths of ~1 m (Lefcheck et al. 2017), as opposed to a 12 m depth limit in more northern areas (DFO 2009). Therefore, eelgrass will be unable to retreat into deeper, cooler waters in Chesapeake Bay with continued warming. If eelgrass habitat is lost, it may be replaced by widgeon grass in shallow waters (Richardson et al. 2018), which has a much higher thermal tolerance (Moore et al. 2014). In some shallow areas of Chesapeake Bay, widgeon grass has had limited colonization after the loss of eelgrass (Moore et al. 2014), but most areas have reverted back to bare substrate (Lefcheck et al. 2017).

The frequency of heatwaves is expected to increase with continued climate change (IPCC 2013). Heatwave events in Chesapeake Bay (Moore et al. 2014) and in the Northeast Atlantic (Reusch et al. 2005) have resulted in immediate negative effects on eelgrass growth and have led to almost complete bed die-offs. As temperatures continue to warm, central-range eelgrass populations along the Northeastern United States and Atlantic Canada will be at greater risk of experiencing heatwaves, yet have lower heat-stress resilience and greater sensitivity than more southern populations (Jueterbock et al. 2016). Furthermore, heatwaves in successive years resulting in complete bed die-offs may permanently destroy perennial eelgrass beds, as the ability to recover through clonal growth would be inhibited in the first year (Jarvis et al. 2012, Lefcheck et al. 2017). Remaining seeds are viable for 1 yr (Orth et al. 2000) but produce seedlings that do not sexually mature for 2 yr; therefore, a second year of heatwaves with complete die-offs would inhibit any natural recovery (Lefcheck et al. 2017). Such short-term heatwave events are not accounted for in our projected LTA of warmer SST, but maintaining high genetic diversity within eelgrass beds, including some genotypes with higher heat tolerance, may help to minimize their impacts (Reusch et al. 2005).

Due to uncertainties in observed present-day climate data (Assis et al. 2018a) and CMIP5 future projections (Bopp et al. 2013) at high latitudes (above the Arctic circle), as well as the under-prediction of present-day habitat in western Hudson Bay and no prediction in Western Greenland, likely due to limited eelgrass occurrence records and a lack of studies, it is difficult to quantitatively calculate the potential for eelgrass northern range expansion. For these reasons, we present maps of the projected distribution of eelgrass by 2100 while limiting our discussion to the general mechanisms for expansion, and expected trends, but do not provide a new northern range limit by the end of the 21st century.

Northern range expansions for eelgrass would be expected as the Arctic continues to warm, as has been projected for the related *Z. noltii* (Valle et al. 2014) and several seaweed species (Assis et al. 2018b, Wilson et al. 2019). Decreasing sea ice coverage would increase the amount of light reaching the seafloor (Krause-Jensen & Duarte 2014). Increasing SST would facilitate reproduction (see Section 4.1) and faster growth rates (Olesen et al. 2015). Laboratory experiments with Greenland eelgrass populations have shown a growth optimum between 20 and 25°C (Beca-Carretero et al. 2018), despite currently being naturally exposed to maximum SST of 15°C (Olesen et al. 2015). Furthermore, eelgrass is able to disperse long distances, as gene flow is still thought to be ongoing from West Atlantic to East Pacific populations (Olsen et al. 2004), and any future range expansions would be made possible by the biotic transport of eelgrass seeds by waterfowl (Sumoski & Orth 2012) or the long-distance dispersal capacity (~150 km) of buoyant reproductive eelgrass shoots (Kendrick et al. 2012). Eelgrass also experienced rapid colonization events following the last glacial maximum into the North Sea (Olsen et al. 2004), suggesting a similar rapid colonization could occur throughout the Canadian Arctic with continued warming. This colonization would be facilitated by the lack of competition with other seagrass species, as eelgrass is the most northerly occurring seagrass (Krause-Jensen & Duarte 2014). However, it would be limited by soft-substrate availability and the impacts of ice-scour (Olesen et al. 2015).

4.3. Implications, caveats, and steps forward

Our SDMs were built using environmental variables that are important for predicting eelgrass distribution under current climate conditions. Yet, there may be a shift in variable importance as these conditions change with rising carbon dioxide (CO_2) concentrations, or as eelgrass adapts or acclimates to changing conditions. Furthermore, while our future projections focus on changes in salinity, temperature, and sea ice, changes in light availability cannot be included, as CMIP5 models do not currently provide projections for DA. Decreasing water clarity has had negative impacts on eelgrass throughout its range in the Northwest Atlantic (Beem & Short 2009, Costello & Kenworthy 2011, Murphy et al. 2019). As SST continues to increase, there will be negative synergistic effects between low light availability and high temperatures, resulting in further decreases in eelgrass abundance (Lefcheck et al. 2017). With the next round of CMIP6, future projections could be improved if future layers of DA become available. Continued climate warming may alter DA values through increases in algal growth or other factors affecting water clarity.

Heat stress also results in decreased production of genes required for pathogen defense and photosynthesis (Jueterbock et al. 2016), which may have important implications for a potential resurgence of the wasting disease in a warmer climate (Burdick et al. 1993). Wasting disease persists in higher salinity waters, and eelgrass is thought to have survived the epidemic in the 1930s by retreating to brackish waters (Short et al. 1986). However, there are additional negative synergistic effects of high temperatures with low salinity (Nejrup & Pedersen 2008) and low oxygen availability (Raun & Borum 2013). SSS was an important driver for the present-day distribution of eelgrass. Eelgrass can tolerate salinities of 10–35‰, with an increase in mortality at 2.5‰ (Nejrup & Pedersen 2008). A warmer climate will result in more freshwater runoff (IPCC 2013), and SSS may therefore have important implications for delimiting the extent of eelgrass throughout the Arctic.

Consequently, projected areas of future habitat with reduced growth should be a management priority, with an aim to limit nutrient runoff and other anthropogenic inputs that may reduce eelgrass habitat suitability in a warming climate. This may be especially important along the southern distribution of eelgrass and in bays or estuaries with high cumulative impacts (Murphy et al. 2019). By limiting the cumulative effects of multiple anthropogenic and natural stressors, the resilience of eelgrass to continued warming may be sustained, thereby ensuring the continued provision of its habitat structure, functions and services to marine ecosystems and human well-being.

While our pixel size and choice of environmental variables were appropriate for modelling at the scale of the entire Northwest Atlantic, future work could develop SDMs within coastal bays or areas denoted with reduced growth, such as Chesapeake Bay. These SDMs should include information about habitat type, depth and other local human impacts to help refine areas for priority management (Murphy et al. 2019). The inclusion of small-scale drivers would help to further refine the estimated habitat area of eelgrass, and the smaller scale may allow for the use of presence–absence algorithms, which would increase our ability to correctly classify absences (Downie et al. 2013). Conversely, future work could also examine whether the projected response to increasing SST would vary if the SDM were built for global populations. Studies in other habitat-forming species have projected greater range shifts when the modelling is performed for genetically distinct regional populations versus global populations (Cacciapaglia & van Woesik 2018). Such future work could use an existing global SDM for eelgrass which has denoted a global present-day predicted habitat (Jayathilake & Costello 2018), to make projections about eelgrass range shifts globally. This could then be compared to the range shifts we calculated for a genetically distinct regional population of eelgrass (Olsen et al. 2004), to examine if there are differences in the projected response with climate change.

On top of increasing SST, climate change is also projected to lead to ocean acidification and sea level rise (Duarte 2002), which will have additional impacts on eelgrass distribution not accounted for in our models. Sea level rise is projected to favour a landward shift of seagrass, following the removal of anthropogenic barriers (Valle et al. 2014). Furthermore, as the concentration of CO_2 increases in seawater, leading to ocean acidification, eelgrass light requirements decrease, leading to increases in vegetative shoot abundance, below-ground biomass, and reproductive output (Palacios & Zimmerman 2007). This increase in CO_2 may be able to partially offset eelgrass higher light requirements with warmer temperatures (Zimmerman et al. 2017). As such, recent studies have examined the potential of using seagrass beds as a carbon sink to increase local pH (Koweek et al. 2018) and suggested their potential for use in carbon mitigation (Duarte et al. 2013), highlighting further benefits to society of protecting and conserving eelgrass beds.

In conclusion, we found that eelgrass beds along the east coast of the USA may experience substantial losses while those within Atlantic Canada and western Greenland will be largely unaffected by continued increases in SST over the 21st century due to climate change. This is good news for the multitude of species that rely on the ecosystem structure and functions provided by eelgrass and the human communities benefiting from the ecosystem services and structure (Schmidt et al. 2011). However, due to the dominance of just one seagrass species in soft-sedimentary habitats of the Northwest Atlantic, minimal range shifts of the northern edge of eelgrass beds may also inhibit northward shifts of associated species, unless they can substitute their current eelgrass habitat with other macrophyte habitats. In comparison, along the southern distribution limit of eelgrass, a southern edge extinction and range shift was projected, even under a strong mitigation scenario. The magnitude of this range shift is uncertain, but it is likely that eelgrass will disappear from at least North Carolina to potentially south of Long Island Sound by 2100. This loss of habitat, and its associated ecosystem functions and services, may be partially offset by a northward shift of shoalgrass, and expansion of widgeon grass habitat.

Acknowledgements. This work was funded by the Canada First Research Excellence Fund Ocean Frontier Institute (OFI): Safe and Sustainable Development of the Ocean Frontier, and the Natural Sciences and Engineering Research Council of Canada (NSERC; grant RGPIN-2014-04491). We acknowledge and thank the contributions of the researchers who developed the Bio-ORACLE marine environmental dataset, the World Climate Research Programme's Working Group on Coupled Modelling (responsible for CMIP5), as well as the modelling groups (described in Section 2.2) for producing and making available their model output.

LITERATURE CITED

Abe M, Kurashima A, Maegawa M (2008) Temperature requirements for seed germination and seedling growth of *Zostera marina* from central Japan. Fish Sci 74: 589–593

Acevedo P, Jiménez-Valverde A, Lobo JM, Real R (2012) Delimiting the geographical background in species distribution modelling. J Biogeogr 39:1383–1390

Assis J, Tyberghein L, Bosch S, Verbruggen H, Serrão EA, De Clerck O (2018a) Bio-ORACLE v2.0: Extending marine data layers for bioclimatic modelling. Glob Ecol Biogeogr 27:277–284

Assis J, Araújo MB, Serrão EA (2018b) Projected climate changes threaten ancient refugia of kelp forests in the North Atlantic. Glob Change Biol 24:e55–e66

Barnett TP, Pierce DW, Schnur R (2001) Detection of anthropogenic climate change in the world's oceans. Science 292:270–274

Barve N, Barve V, Jiménez-Valverde A, Lira-Noriega A and others (2011) The crucial role of the accessible area in ecological niche modeling and species distribution modeling. Ecol Modell 222:1810–1819

Beca-Carretero P, Olesen B, Marbà N, Krause-Jensen D (2018) Response to experimental warming in northern eelgrass populations: comparison across a range of temperature adaptations. Mar Ecol Prog Ser 589:59–72

Beem NT, Short FT (2009) Subtidal eelgrass declines in the Great Bay Estuary, New Hampshire and Maine, USA. Estuar Coast 32:202–205

Biebl R, McRoy CP (1971) Plasmatic resistance and rate of respiration and photosynthesis of *Zostera marina* at different salinities and temperatures. Mar Biol 8:48–56

Bopp L, Resplandy L, Orr JC, Doney SC and others (2013) Multiple stressors of ocean ecosystems in the 21st century: projections with CMIP5 models. Biogeosciences 10: 6225–6245

Bos AR, Bouma TJ, de Kort GLJ, van Katwijk MM (2007) Ecosystem engineering by annual intertidal seagrass beds: sediment accretion and modification. Estuar Coast Shelf Sci 74:344–348

Bosch S, Tyberghein L, De Clerck O (2018) 'sdmpredictors': Species distribution modelling predictor datasets. R package version 0.2.6.

Burdick DM, Short FT, Wolf J (1993) An index to access and monitor the progression of wasting disease in eelgrass *Zostera marina*. Mar Ecol Prog Ser 94:83–90

Cacciapaglia C, van Woesik R (2018) Marine species distribution modelling and the effects of genetic isolation under climate change. J Biogeogr 45:154–163

Churchill AC, Riner MI (1978) Anthesis and seed production in *Zostera marina* L. from Great South Bay, New York, USA. Aquat Bot 4:83–93

Clausen KK, Krause-Jensen D, Olesen B, Marbà N (2014) Seasonality of eelgrass biomass across gradients in temperature and latitude. Mar Ecol Prog Ser 506:71–85

Costello CT, Kenworthy WJ (2011) Twelve-year mapping and change analysis of eelgrass (*Zostera marina*) areal abundance in Massachusetts (USA) identifies statewide declines. Estuar Coast 34:232–242

Cottam C, Munro DA (1954) Eelgrass status and environmental relations. J Wildl Manag 18:449–460

De Cock AWAM (1981) Influence of temperature and variations in temperature on flowering in *Zostera marina* L. under laboratory conditions. Aquat Bot 10:125–131

DFO (2009) Does eelgrass (*Zostera marina*) meet the criteria as an ecologically significant species? DFO Can Sci Advis Sec Sci Advis Rep 2009:1–11

Downie AL, Von Numers M, Boström C (2013) Influence of model selection on the predicted distribution of the seagrass *Zostera marina*. Estuar Coast Shelf Sci 121–122: 8–19

Duarte CM (2002) The future of seagrass meadows. Environ Conserv 29:192–206

Duarte CM, Losada IJ, Hendriks IE, Mazarrasa I, Marbà N (2013) The role of coastal plant communities for climate change mitigation and adaptation. Nat Clim Chang 3: 961–968

Dufresne JL, Foujols MA, Denvil S, Caubel A and others (2013) Climate change projections using the IPSL-CM5 Earth System Model: from CMIP3 to CMIP5. Clim Dyn 40:2123–2165

Dunne JP, John JG, Adcroft AJ, Griffies SM and others (2012) GFDL's ESM2 global coupled climate-carbon earth system models. I. Physical formulation and baseline simulation characteristics. J Clim 25:6646–6665

Elith J, Graham CH, Anderson RP, Dudik M and others (2006) Novel methods improve prediction of species' distributions from occurrence data. Ecography 29: 129–151

Elith J, Kearney MR, Phillips SJ (2010) The art of modelling range-shifting species. Methods Ecol Evol 1:330–342

Green E, Short FT (2003) World atlas of seagrasses. University of California Press, Berkeley

Hansen J, Sato M, Ruedy R, Lo K, Lea DW, Medina-Elizade M (2006) Global temperature change. Proc Natl Acad Sci USA 103:14288–14293

Hijmans RJ, Phillips SJ, Leathwick JR, Elith J (2017) 'dismo': Species distribution modeling. R package version 1.1-4

Hughes L (2000) Biological consequences of global warming: Is the signal already apparent? Trends Ecol Evol 15: 56–61

Infantes E, Eriander L, Moksnes PO (2016) Eelgrass (*Zostera marina*) restoration on the west coast of Sweden using seeds. Mar Ecol Prog Ser 546:31–45

IPCC (2013) Climate change 2013: the physical science basis. Contribution of working group I to the fifth assessment report of the Intergovernmental Panel on Climate Change. Cambridge University Press, Cambridge

Jarvis JC, Moore KA, Kenworthy WJ (2012) Characterization and ecological implication of eelgrass life history strategies near the species' southern limit in the western North Atlantic. Mar Ecol Prog Ser 444:43–56

Jayathilake DRM, Costello MJ (2018) A modelled global distribution of the seagrass biome. Biol Conserv 226: 120–126

Jueterbock A, Franssen SU, Bergmann N, Gu J and others (2016) Phylogeographic differentiation versus transcriptomic adaptation to warm temperatures in *Zostera marina*, a globally important seagrass. Mol Ecol 25: 5396–5411

Kendrick GA, Waycott M, Carruthers TJB, Cambridge ML and others (2012) The central role of dispersal in the maintenance and persistence of seagrass populations. Bioscience 62:56–65

Kohavi R (1995) A study of cross-validation and bootstrap for accuracy estimation and model selection. Int Jt Conf Artif Intell 14:1137–1143

Kotta J, Möller T, Orav-Kotta H, Pärnoja M (2014) Realized niche width of a brackish water submerged aquatic vegetation under current environmental conditions and projected influences of climate change. Mar Environ Res 102:88–101

Koweek DA, Zimmerman RC, Hewett KM, Gaylord B and others (2018) Expected limits on the ocean acidification buffering potential of a temperate seagrass meadow. Ecol Appl 28:1694–1714

Krause-Jensen D, Duarte CM (2014) Expansion of vegetated coastal ecosystems in the future Arctic. Front Mar Sci 1: 1–10

Lalumière R, Messier D, Fournier JJ, Peter McRoy C (1994) Eelgrass meadows in a low arctic environment, the northeast coast of James Bay, Québec. Aquat Bot 47: 303–315

Lee KS, Park SR, Kim YK (2007) Effects of irradiance, temperature, and nutrients on growth dynamics of seagrasses: a review. J Exp Mar Biol Ecol 350:144–175

Lefcheck JS, Wilcox DJ, Murphy RR, Marion SR, Orth RJ (2017) Multiple stressors threaten the imperiled coastal foundation species eelgrass (*Zostera marina*) in Chesapeake Bay, USA. Glob Change Biol 23:3474–3483

Lefcheck JS, Orth RJ, Dennison WC, Wilcox DJ and others (2018) Long-term nutrient reductions lead to the unprecedented recovery of a temperate coastal region. Proc Natl Acad Sci USA 115:3658–3662

Liu C, Newell G, White M (2016) On the selection of thresholds for predicting species occurrence with presence-only data. Ecol Evol 6:337–348

Mallin MA, Burkholder JM, Cahoon LB, Posey MH (2000) North and South Carolina Coasts. Mar Pollut Bull 41: 56–75

Martínez B, Arenas F, Trilla A, Viejo RM, Carreño F (2015) Combining physiological threshold knowledge to species distribution models is key to improving forecasts of the future niche for macroalgae. Glob Change Biol 21: 1422–1433

Micheli F, Bishop MJ, Peterson CH, Rivera J (2008) Alteration of seagrass species composition and function over the past two decades. Ecol Monogr 78:225–244

Moore KA, Shields E, Parrish D, Orth RJ (2012) Eelgrass survival in two contrasting systems: role of turbidity and summer water temperatures. Mar Ecol Prog Ser 448: 247–258

Moore KA, Shields EC, Parrish DB (2014) Impacts of varying estuarine temperature and light conditions on *Zostera marina* (eelgrass) and its interactions with *Ruppia maritima* (widgeongrass). Estuar Coast 37:20–30

Moss RH, Edmonds JA, Hibbard KA, Manning MR and others (2010) The next generation of scenarios for climate change research and assessment. Nature 463:747–756

Murphy GEP, Wong M, Lotze HK (in press) (2019) A human impact metric for coastal ecosystems with application to seagrass beds in Atlantic Canada. Facets 4:210–237

Naimi B, Hamm NAS, Groen TA, Skidmore AK, Toxopeus AG (2014) Where is positional uncertainty a problem for species distribution modelling? Ecography 37:191–203

Nejrup LB, Pedersen MF (2008) Effects of salinity and water temperature on the ecological performance of *Zostera marina*. Aquat Bot 88:239–246

Nelson WG (2009) Seagrasses and protective criteria: a review and assessment of research status. Office of Research and Development, National Health and Environmental Effects Research Laboratory, EPA/600/R-09/050

Olesen B, Krause-Jensen D, Marbà N, Christensen PB (2015) Eelgrass *Zostera marina* in subarctic Greenland: Dense meadows with slow biomass turnover in cold waters. Mar Ecol Prog Ser 518:107–121

Olsen JL, Stam WT, Coyer JA, Reusch TBH and others (2004) North Atlantic phylogeography and large-scale population differentiation of the seagrass *Zostera marina* L. Mol Ecol 13:1923–1941

Orth RJ, Harwell MC, Bailey EM, Bartholomew A and others (2000) A review of issues in seagrass seed dormancy and germination: implications for conservation and restoration. Mar Ecol Prog Ser 200:277–288

Palacios SL, Zimmerman RC (2007) Response of eelgrass *Zostera marina* to CO_2 enrichment: possible impacts of climate change and potential for remediation of coastal habitats. Mar Ecol Prog Ser 344:1–13

Pershing AJ, Alexander MA, Hernandez CM, Kerr LA and others (2015) Slow adaptation in the face of rapid warm-

ing leads to collapse of the Gulf of Maine cod fishery. Science 350:809–812

Phillips SJ, Dudík M, Schapire RE (2004) A maximum entropy approach to species distribution modeling. Proc 21st Intl Conf Mach Learn 21:655–662

Phillips SJ, Anderson RP, Schapire RE (2006) Maximum entropy modeling of species geographic distributions. Ecol Modell 190:231–259

Poloczanska ES, Brown CJ, Sydeman WJ, Kiessling W and others (2013) Global imprint of climate change on marine life. Nat Clim Chang 3:919–925

Porsild AE (1932) Notes on the occurrence of *Zostera* and *Zannichellia* in Arctic North America. Rhodora 34:90–94

R Core Team (2018) R: a language and environment for statistical computing. R Foundation for Statistical Computing, Vienna. www.r-project.org/

Raun AL, Borum J (2013) Combined impact of water column oxygen and temperature on internal oxygen status and growth of *Zostera marina* seedlings and adult shoots. J Exp Mar Biol Ecol 441:16–22

Reusch TBH, Ehlers A, Hammerli A, Worm B (2005) Ecosystem recovery after climatic extremes enhanced by genotypic diversity. Proc Natl Acad Sci USA 102:2826–2831

Richardson JP, Lefcheck JS, Orth RJ (2018) Warming temperatures alter the relative abundance and distribution of two co-occurring foundational seagrasses in Chesapeake Bay, USA. Mar Ecol Prog Ser 599:65–74

Schmidt AL, Coll M, Romanuk TN, Lotze HK (2011) Ecosystem structure and services in eelgrass *Zostera marina* and rockweed *Ascophyllum nodosum* habitats. Mar Ecol Prog Ser 437:51–68

Serebryakova A (2017) Acclimation and adaptation of invasive seaweeds—a case study with the brown alga *Sargassum muticum*. PhD thesis, Universidade do Algarve, Faro

Short FT, Mathieson AC, Nelson JI (1986) Recurrence of the eelgrass wasting disease at the border of New Hampshire and Maine, USA. Mar Ecol Prog Ser 29:89–92

Short FT, Polidoro BA, Livingstone SR, Carpenter KE and others (2011) Extinction risk assessment of the world's seagrass species. Biol Conserv 144:1961–1971

Sumoski SE, Orth RJ (2012) Biotic dispersal in eelgrass *Zostera marina*. Mar Ecol Prog Ser 471:1–10

Taylor KE, Stouffer RJ, Meehl GA (2012) An overview of CMIP5 and the experiment design. Bull Am Meteorol Soc 93:485–498

Tyberghein L, Verbruggen H, Pauly K, Troupin C, Mineur F, De Clerck O (2012) Bio-ORACLE: A global environmental dataset for marine species distribution modelling. Glob Ecol Biogeogr 21:272–281

Valle M, van Katwijk MM, de Jong DJ, Bouma TJ and others (2013) Comparing the performance of species distribution models of *Zostera marina*: implications for conservation. J Sea Res 83:56–64

Valle M, Chust G, del Campo A, Wisz MS, Olsen SM, Garmendia JM, Borja Á (2014) Projecting future distribution of the seagrass *Zostera noltii* under global warming and sea level rise. Biol Conserv 170:74–85

Waycott M, Duarte CM, Carruthers TJB, Orth RJ and others (2009) Accelerating loss of seagrasses across the globe threatens coastal ecosystems. Proc Natl Acad Sci USA 106:12377–12381

Wilson KL, Skinner MA, Lotze HK (2019) Projected 21st-century distribution of canopy forming seaweeds in the Northwest Atlantic with climate change. Divers Distrib 25:582–602

Zimmerman RC, Hill VJ, Gallegos CL (2015) Predicting effects of ocean warming, acidification, and water quality on Chesapeake region eelgrass. Limnol Oceanogr 60: 1781–1804

Zimmerman RC, Hill VJ, Jinuntuya M, Celebi B and others (2017) Experimental impacts of climate warming and ocean carbonation on eelgrass *Zostera marina*. Mar Ecol Prog Ser 566:1–15

Editorial responsibility: Lisandro Benedetti-Cecchi, Pisa, Italy

Submitted: September 3, 2018; Accepted: April 17, 2019
Proofs received from author(s): June 7, 2019